JACS ARTICLES

Published on Web 12/13/2010

Heparin Binding by Murine Recombinant Prion Protein Leads to Transient Aggregation and Formation of RNA-Resistant Species

Tuane C. R. G. Vieira,[†] Daniel P. Reynaldo,[†] Mariana P. B. Gomes,[†] Marcius S. Almeida,[†] Yraima Cordeiro,[‡] and Jerson L. Silva*[,†]

Instituto de Bioquímica Médica, Instituto Nacional de Ciência e Tecnologia de Biologia Estrutural e Bioimagem and Faculdade de Farmácia, Universidade Federal do Rio de Janeiro 21491-902

Received August 1, 2010; E-mail: jerson@bioqmed.ufrj.br

Abstract: The conversion of cellular prion protein (PrP^C) into the pathological conformer PrP^{Sc} requires contact between both isoforms and probably also requires a cellular factor, such as a nucleic acid or a glycosaminoglycan (GAG). Little is known about the structural features implicit in the GAG−PrP interaction. In the present work, light scattering, fluorescence, circular dichroism, and nuclear magnetic resonance (NMR) spectroscopy were used to describe the chemical and physical properties of the murine recombinant PrP 23-231 interaction with low molecular weight heparin (LMWHep) at pH 7.4 and 5.5. LMWHep interacts with rPrP 23-231, thereby inducing transient aggregation. The interaction between murine rPrP and heparin at pH 5.5 had a stoichiometry of 2:1 (LMWHep:rPrP 23-231), in contrast to a 1:1 binding ratio at pH 7.4. At binding equilibrium, NMR spectra showed that rPrP complexed with LMWHep had the same general fold as that of the free protein, even though the binding can be indicated by significant changes in few residues of the C-terminal domain, especially at pH 5.5. Notably, the soluble LMWHep:rPrP complex prevented RNA-induced aggregation. We also investigated the interaction between LMWHep and the deletion mutants rPrP Δ51-90 and Δ32-121. Heparin did not bind these constructs at pH 7.4 but was able to interact at pH 5.5, indicating that this glycosaminoglycan binds the octapeptide repeat region at pH 7.4 but can also bind other regions of the protein at pH 5.5. The interaction at pH 5.5 was dependent on histidine residues of the murine rPrP 23-231. Depending on the cellular milieu, the PrP may expose different regions that can bind GAG. These results shed light on the role of GAGs in PrP conversion. The transient aggregation of PrP may explain why some GAGs have been reported to induce the conversion into the misfolded, scrapie conformation, whereas others are thought to protect against conversion. The acquired resistance of the complex against RNA-induced aggregation explains some of the unique properties of the PrP interaction with GAGs.

Introduction

Transmissible spongiform encephalopathies (TSEs), such as Creutzfeldt−Jakob disease in humans, scrapie in sheep, and bovine spongiform encephalopathy in cattle, are fatal degenerative diseases that are caused by prions.[1] The cellular isoform of a prion protein is a glycoprotein attached outside to the cell surface via a glycosylphosphatidylinositol (GPI) anchor at the protein's C-terminus and is highly expressed in cells of the central nervous system.[2] In healthy, noninfected cells, the cellular prion protein (PrP^C) is mainly composed of α-helices that are linked to a disordered N-terminal domain.[3−5] The refolding of PrP^C into an abnormal β-sheet-rich isoform that is capable of forming toxic and infectious aggregates, called PrP scrapie (PrP^{Sc}), is the key event in prion disease pathology.[6,7] Although it is well-established, it is still unclear how this process results in neuronal cell death.

According to the protein-only hypothesis, PrP^{Sc} acts as a template, inducing the conversion of PrP^C and propagating itself as an 'infectious protein'.[8,9] The conversion occurs primarily on the cell surface or in endocytic vesicles.[10−12] The scrapie isoform is thermodynamically more stable than the native PrP. A large energetic barrier, which is associated with partial

* Corresponding author.
† Instituto de Bioquímica Médica.
‡ Faculdade de Farmácia.

(1) Knight, R. S.; Will, R. G. *J. Neurol., Neurosurg. Psychiatry* **2004**, *75* (Suppl 1), i36–42.
(2) Stahl, N.; Borchelt, D. R.; Hsiao, K.; Prusiner, S. B. *Cell* **1987**, *51*, 229–240.
(3) Liu, H.; Farr-Jones, S.; Ulyanov, N. B.; Llinas, M.; Marqusee, S.; Groth, D.; Cohen, F. E.; Prusiner, S. B.; James, T. L. *Biochemistry* **1999**, *38*, 5362–77.
(4) Donne, D. G.; Viles, J. H.; Groth, D.; Mehlhorn, I.; James, T. L.; Cohen, F. E.; Prusiner, S. B.; Wright, P. E.; Dyson, H. J. *Proc. Natl. Acad. Sci. U.S.A.* **1997**, *94*, 13452–13457.
(5) Zahn, R.; Liu, A.; Luhrs, T.; Riek, R.; von Schroetter, C.; Lopez, G. F.; Billeter, M.; Calzolai, L.; Wider, G.; Wuthrich, K. *Proc. Natl. Acad. Sci. U.S.A.* **2000**, *97*, 145–150.
(6) Pan, K. M.; Baldwin, M.; Nguyen, J.; Gasset, M.; Serban, A.; Groth, D.; Mehlhorn, I.; Huang, Z.; Fletterick, R. J.; Cohen, F. E. *Proc. Natl. Acad. Sci. U.S.A.* **1993**, *90*, 10962–10966.
(7) Caughey, B. W.; Dong, A.; Bhat, K. S.; Ernst, D.; Hayes, S. F.; Caughey, W. S. *Biochemistry* **1991**, *30*, 7672–7680.
(8) Cohen, F. E.; Prusiner, S. B. *Annu. Rev. Biochem.* **1998**, *67*, 793–819.
(9) Prusiner, S. B. *Proc. Natl. Acad. Sci. U.S.A.* **1998**, *95*, 13363–13383.

10.1021/ja106725p

unfolding and oligomerization, separates PrP^{C} from PrP^{Sc}.[13,14] Although prion diseases are believed to occur through an autocatalytic process, it seems likely that other molecules are crucial for prion propagation, acting as adjuvant factors by lowering this free-energy barrier.[15−17] The different in vivo environments of the protein are likely to influence its ability to misfold and aggregate. Several candidate cofactors have been proposed, such as cellular adhesion molecules,[18,19] nucleic acids,[20−23] and glycosaminoglycans (GAGs).[23−25]

GAGs are primary components of the cell surface and cell−extracellular matrix interface. They are linear polysaccharides composed of a disaccharide repeat unit of a hexuronic acid linked to a hexosamine and are mainly modified by *N*-deacetylase and *N*-sulfotransferases.[26] Sulfated GAGs, particularly heparan sulfate, have long been implicated in interactions with amyloidogenic proteins and are associated with several important diseases.[27−30] Several studies have linked heparan sulfate (HS) or its analog heparin to the pathogenesis and metabolism of prions.[23−25,31,32] For example, it has been reported that HS accumulates in cerebral prion amyloid plaques[33] and stimulates the cell-free conversion of PrP^{C} to PrP^{res} (resistant PrP).[32] In addition, HS is necessary for PrP^{Sc} formation in ScN2a cells[25] and may act as its cell-surface receptor.[24] Sulfated GAGs have also been shown to prevent the accumulation of protease-resistant prions.[34,35]

Heparin has been shown to bind bovine recombinant PrP^{C}; this interaction was strongest at acidic pH values and sharply decreased at pH values above 7.5.[36] At pH 6.5, the interaction was followed by the formation of PrP oligomeric complexes.[31] Although direct interactions between the mammalian prion protein and heparin have been demonstrated, little is known about the structural features of this association.

Investigations of the heparin binding site of PrP^{C} using synthetic peptides and biosensor analysis have revealed the involvement of residues in three segments of the N-terminal sequence with independent binding activities: the highly cationic amino-terminal residues (23−52), the octapeptide repeats (53−93), and a more C-terminal site (110−128).[37] Conversely, Yin and collaborators reported that when the first 12 amino acids of the N-terminus of human recombinant prion protein were deleted, the recombinant protein was no longer able to bind GAG.[38] Consequently, there is ongoing debate regarding which residues are the most important for binding.

In an attempt to characterize the structural changes induced by LMWHep on rPrP 23-231 and to identify the binding sites that are important for this interaction, we first established that LMWHeparin interacts with murine recombinant prion protein in a pH-dependent manner; binding is stronger at acidic pH. Results obtained with a PrP mutant lacking a region of the N-terminal domain led us to conclude that heparin interacts with the octapeptide repeat region at pH 7.4; however, at acidic pH values, rPrP 23-231 exhibits two binding regions, where binding is mediated by histidine residues. The most striking finding was that LMWHep induces the transient aggregation of PrP, which evolves into a soluble LMWHep−PrP complex. Nuclear magnetic resonance (NMR) results show that the prion protein complexed with LMWHep has the same general fold as the free protein. We observed only a few chemical shift deviations of the N- and C-terminal amino acids, indicating that in the nonaggregated complex, this interaction does not form a scrapie-like isoform. Notably, the Hep−rPrP complex is immune to RNA-induced aggregation.

Materials and Methods

Prion Protein, Low Molecular Weight Heparin, and RNA Samples. The recombinant full-length PrP 23-231 and the N-terminal deletion mutants rPrP Δ51-90 and rPrPΔ32-121 were expressed in *Escherichia coli* and purified by high-affinity column refolding, as described previously.[39] LMWHep (average wt of 3000 Da, cat. no. H3400) was obtained from Sigma-Aldrich (St. Louis, MO). Total RNA was extracted from cultured neuroblastoma (N2a) cells (N2aRNA) using the RNeasy Midikit (QIAGEN, Fremont, CA) and the RNAspin Mini isolation kit (GE Healthcare, Milwaukee, WI).

Spectroscopic Measurements. Light scattering (LS) spectra were recorded on a PC1 spectrofluorimeter (ISS, Champaign, IL) in an "L" geometry (at 90° relative to the excitation light), illuminating the samples at 320 nm and collecting LS from 300 to 340 nm. Oligomerization of rPrP 23-231 was followed by monitoring LS after the addition of LMWHep (steady-state measurments were taken after 6 s). For the assays of disaggregation kinetics, protein solutions were pre-equilibrated before LMWHep was added,

(10) Borchelt, D. R.; Taraboulos, A.; Prusiner, S. B. *J. Biol. Chem.* **1992**, *267*, 16188–16199.
(11) Caughey, B.; Raymond, G. J. *J. Biol. Chem.* **1991**, *266*, 18217–18223.
(12) Caughey, B.; Raymond, G. J.; Ernst, D.; Race, R. E. *J.Virol.* **1991**, *65*, 6597–6603.
(13) Cohen, F. E. *J. Mol. Biol.* **1999**, *293*, 313–320.
(14) Harrison, P. M.; Chan, H. S.; Prusiner, S. B.; Cohen, F. E. *J. Mol. Biol.* **1999**, *286*, 593–606.
(15) Telling, G. C.; Scott, M.; Mastrianni, J.; Gabizon, R.; Torchia, M.; Cohen, F. E.; DeArmond, S. J.; Prusiner, S. B. *Cell* **1995**, *83*, 79–90.
(16) Caughey, B.; Baron, G. S. *Nature* **2006**, *443*, 803–810.
(17) Silva, J. L.; Lima, L. M.; Foguel, D.; Cordeiro, Y. *Trends Biochem. Sci.* **2008**, *33*, 132–140.
(18) Vana, K.; Weiss, S. *J. Mol. Biol.* **2006**, *358*, 57–66.
(19) Gauczynski, S.; Peyrin, J. M.; Haik, S.; Leucht, C.; Hundt, C.; Rieger, R.; Krasemann, S.; Deslys, J. P.; Dormont, D.; Lasmezas, C. I.; Weiss, S. *EMBO J.* **2001**, *20*, 5863–5875.
(20) Gomes, M. P.; Millen, T. A.; Ferreira, P. S.; e Silva, N. L.; Vieira, T. C.; Almeida, M. S.; Silva, J. L.; Cordeiro, Y. *J. Biol. Chem.* **2008**, *283*, 19616–25.
(21) Cordeiro, Y.; Machado, F.; Juliano, L.; Juliano, M. A.; Brentani, R. R.; Foguel, D.; Silva, J. L. *J. Biol. Chem.* **2001**, *276*, 49400–49409.
(22) Cordeiro, Y.; Silva, J. L. *Protein Pept. Lett.* **2005**, *12*, 251–255.
(23) Deleault, N. R.; Geoghegan, J. C.; Nishina, K.; Kascsak, R.; Williamson, R. A.; Supattapone, S. *J. Biol. Chem.* **2005**, *280*, 26873–26879.
(24) Horonchik, L.; Tzaban, S.; Ben Zaken, O.; Yedidia, Y.; Rouvinski, A.; Papy-Garcia, D.; Barritault, D.; Vlodavsky, I.; Taraboulos, A. *J. Biol. Chem.* **2005**, *280*, 17062–17067.
(25) Ben Zaken, O.; Tzaban, S.; Tal, Y.; Horonchik, L.; Esko, J. D.; Vlodavsky, I.; Taraboulos, A. *J. Biol. Chem.* **2003**, *278*, 40041–40049.
(26) Sasisekharan, R.; Raman, R.; Prabhakar, V. *Annu. Rev. Biomed. Eng* **2006**, *8*, 181–231.
(27) Scholefield, Z.; Yates, E. A.; Wayne, G.; Amour, A.; McDowell, W.; Turnbull, J. E. *J. Cell Biol.* **2003**, *163*, 97–107.
(28) Schubert, D.; Schroeder, R.; LaCorbiere, M.; Saitoh, T.; Cole, G. *Science* **1988**, *241*, 223–226.
(29) Lindahl, B.; Lindahl, U. *J. Biol. Chem.* **1997**, *272*, 26091–26094.
(30) Ancsin, J. B. *Amyloid* **2003**, *10*, 67–79.
(31) Gonzalez-Iglesias, R.; Pajares, M. A.; Ocal, C.; Espinosa, J. C.; Oesch, B.; Gasset, M. *J. Mol. Biol.* **2002**, *319*, 527–540.
(32) Wong, C.; Xiong, L. W.; Horiuchi, M.; Raymond, L.; Wehrly, K.; Chesebro, B.; Caughey, B. *EMBO J.* **2001**, *20*, 377–386.
(33) Snow, A. D.; Wight, T. N.; Nochlin, D.; Koike, Y.; Kimata, K.; DeArmond, S. J.; Prusiner, S. B. *Lab. Invest.* **1990**, *63*, 601–611.
(34) Priola, S. A.; Caughey, B. *Mol. Neurobiol.* **1994**, *8*, 113–120.
(35) Caughey, B.; Brown, K.; Raymond, G. J.; Katzenstein, G. E.; Thresher, W. *J. Virol.* **1994**, *68*, 2135–2141.
(36) Andrievskaia, O.; Potetinova, Z.; Balachandran, A.; Nielsen, K. *Arch. Biochem. Biophys.* **2007**, *460*, 10–16.
(37) Warner, R. G.; Hundt, C.; Weiss, S.; Turnbull, J. E. *J. Biol. Chem.* **2002**, *277*, 18421–18430.
(38) Yin, S.; Yu, S.; Li, C.; Wong, P.; Chang, B.; Xiao, F.; Kang, S. C.; Yan, H.; Xiao, G.; Grassi, J.; Tien, P.; Sy, M. S. *J. Biol. Chem.* **2006**, *281*, 10698–10705.
(39) Zahn, R.; von, S. C.; Wuthrich, K. *FEBS Lett.* **1997**, *417*, 400–404.

and LS was monitored at 320 nm as a function of time. The data were fit by a double exponential decay to acquire rate constants and amplitudes for the fast and slow phases. For anisotropy measurements, samples were excited at 280 nm, and emission was observed through a WG335 filter. The results represent the means of three individual measurements for each experiment. All experiments were performed at room temperature.

Fast Kinetic Experiments. An SX17MV stopped-flow apparatus from Applied Photophysics was used for the fast kinetic experiments. The samples were placed in appropriate syringes, and a nitrogen pulse was applied to eject 50 μL from each syringe (100 μL total) into a cuvette. The sample was excited at 295 nm for protein fluorescence analysis and at 360 nm for LS. Emission spectra were collected through a 320 nm long-pass filter. The signal was detected by a photomultiplier at 90° to the incident light. Five shots were performed for each point, and the signals were analyzed with the Pro Data viewer software provided by Applied Photophysics. The rate constants and the amplitude were obtained by adjusting a single exponential to the signal. Then, the data were analyzed by considering a simple two-state reversible equilibrium between rPrP 23-231 and LMWHep, according to the following scheme:

$$\mathrm{PrP} + \mathrm{LMWHep} \rightleftarrows \mathrm{PrP-LMWHep}$$

where PrP is the free protein, LMWHep is free heparin, and PrP−LMWHep is the protein bound to LMWHep. The K_d values and the number of binding sites were calculated using the following equation:[40,41]

$$\Delta F/\Delta F_{max} = n\mathrm{PrP_o} + X\mathrm{i} + K_d - [(n\mathrm{PrP_o} + X\mathrm{i} + K_d)^2 - 4n\mathrm{PrP_o}X\mathrm{i})^{1/2}]/2n\mathrm{PrP_o} \quad (1)$$

where $\mathrm{PrP_o}$ is the initial concentration of rPrP 23-231 (constant), Xi is the initial concentration of LMWHep (varied), ΔF is the difference between the observed fluorescence amplitude and the minimum fluorescence amplitude, and ΔF_{max} is the difference between the maximal and minimal fluorescence amplitudes. K_d is the dissociation constant, F_{max} is the maximum fluorescence signal, and n is the number of binding sites per molecule.

Far-UV Circular Dichroism. Circular dichroism (CD) spectra of rPrP 23-231 were recorded on a Jasco J-715 spectropolarimeter (Jasco Corporation, Tokyo, Japan) with 0.01 and 0.02 cm circular path length cells at 25 °C. All spectra had the spectrum of the buffer or heparin solution subtracted. Four trials were collected per experiment, and each experiment was repeated three times.

NMR Experiments. NMR spectra were collected at 298 K with a Bruker Avance 800 MHz spectrometer equipped with gradient triple resonance probes, with 0.2 mM uniformly labeled [^{15}N]rPrP 23-231 in 20 mM sodium phosphate buffer (pH 7.4) or 20 mM sodium acetate buffer (pH 5.5), 100 mM NaCl, and a 10% D_2O/90% H_2O mixture in the presence (1:1 molar ratio) or absence of LMWHep. The spectra were processed using TOPSPIN 2.1 (Bruker) and analyzed with CARA 1.8.[42] The identification of some spin systems in the 2D [^{1}H,^{15}N] heteronuclear single quantum correlation (HSQC) spectra was done using the resonance assignment of mPrP(121-231) at pH 4.5, kindly provided by Dr. Kurt Wüthrich and Dr. Simone Hornemann from the Institute of Molecular Biology and Biophysics, ETH, Zürich, and the PrP tridimensional structure was based on data from PDB 1XYX. Two-dimensional [^{15}N,^{1}H] HSQC spectra were collected with 2048 × 200 points and 8−220 scans for the different samples. Combined chemical shift changes were calculated using the following equation:[43]

$$\Delta\delta_{comb} = \{[(\Delta\delta_{NH})^2 + (\Delta\delta_N \times 0.15)^2]/2\}^{1/2} \quad (2)$$

Diethylpyrocarbonate (DEPC) Modification of rPrP 23-231. N-carbethoxylation of histidine residues was carried out using DEPC, according to a previously described protocol with some modifications.[44] First, a saturation curve with DEPC was performed with 2 μM rPrP 23-231 in 10 mM sodium acetate, 100 mM NaCl (pH 5.5) by monitoring the absorbance at 240 nm. The reaction reached saturation with 8 mM DEPC (see the Supporting Information, Figure S1). On the day of use, an aliquot of DEPC was added to a 2 μM rPrP 23-231 solution to a final concentration of 10 mM. After 30 min at room temperature, increasing concentrations of LMWHep were added to DEPC treated and untreated samples, and light scattering measurements were taken.

Results

Murine rPrP 23-231 Interaction with LMWHep. Glycosaminoglycans such as heparan sulfate have been suggested to be cellular receptors for infectious prions,[24,25] and direct interactions between PrP and sulfated glycans have been documented.[31,32,36,45] Heparin, an analog of HS, was shown to bind the bovine prion protein at acidic pH values.[31,36] To investigate the binding of LMWHep to the murine prion protein, we conducted fluorescence anisotropy measurements of rPrP 23-231 with increasing concentrations of LMWHep at two different pH values (pH 7.4 and 5.5), as shown in Figure 1. We followed the anisotropy of rPrP tryptophan residues (at 280 nm) upon LMWHep addition. An increase in anisotropy values reflects the increase in the molecular size of rPrP as well as decrease in the local mobility of the Trp residues,[46] indicating, in this case, the binding of LMWHep to the protein. The increased anisotropy values confirmed LMWHep:rPrP 23-231 complex formation at acidic and neutral pH values. Saturation was reached at a molar ratio of approximately 1:1 (LMWHep:rPrP 23-231) at pH 7.4 and 2:1 (LMWHep:rPrP 23-231) at pH 5.5 (Figure 1), as can be seen through the drawn vertical lines in Figure 1.

Effect of LMWHep on Protein Secondary Structure and Aggregation. Using CD, we investigated whether heparin could induce structural changes in the prion protein, leading to a scrapie conformation or an intermediate of the conversion process. Murine rPrP 23-231 exhibited typical α-helical far-UV CD spectra, with minima at 222 and 208 nm (Figure 2A inset). Increasing heparin concentrations led to a decrease in ellipticity at pH 5.5 and 7.4 (Figure 2A shows changes at 222 nm). We also evaluated the protein oligomeric state using LS measurements and found that an increase in LMWHep concentration was accompanied by increased light scattering values, suggesting the formation of oligomers/aggregates. More oligomerization/aggregation occurred at pH 5.5 (Figure 2B). Transmission electron microscopy analysis showed that these aggregates have a bell-shaped morphology (see Supporting Information, Figure S2).

To further analyze PrP:LMWHep complex formation, we performed fast kinetic measurements with different LMWHep concentrations and monitored changes in fluorescence and light scattering. For all LMWHep concentrations, we observed an increase in fluorescence intensity (not shown) and light scattering

(40) Lima, L. M.; Silva, J. L. *J. Biol. Chem.* **2004**, *279*, 47968–47974.
(41) Ingraham, R. H.; Swenson, C. A. *J. Biol. Chem.* **1984**, *259*, 9544–8.
(42) Keller, R. *Diss*; Swiss Federal Institute of Technology: Zurich, 2005.
(43) Mulder, F. A.; Schipper, D.; Bott, R.; Boelens, R. *J. Mol. Biol.* 1999.
(44) Hesp, J. R.; Raven, N. D.; Sutton, J. M. *Biochem. Biophys. Res. Commun.* **2007**, *362*, 695–699.
(45) Yin, S.; Pham, N.; Yu, S.; Li, C.; Wong, P.; Chang, B.; Kang, S. C.; Biasini, E.; Tien, P.; Harris, D. A.; Sy, M. S. *Proc. Natl. Acad. Sci. U.S.A.* **2007**, *104*, 7546–7551.
(46) Lakowicz, J. R. *Principles of fluorescence spectroscopy*; Kluwer Academic/Plenum publishers: New York, 1999.

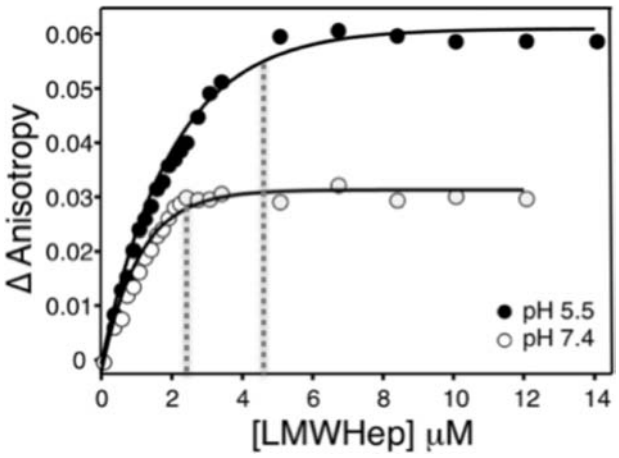

Figure 1. Binding of the murine prion protein to LMWHeparin at two different pH values and with the addition of increasing concentrations of LMWHep to 2 μM rPrP 23-231. Binding was monitored by tryptophan fluorescence anisotropy at 280 nm. Experiments were performed in 10 mM Tris and 100 mM NaCl (pH 7.4) or 10 mM sodium acetate and 100 mM NaCl (pH 5.5).

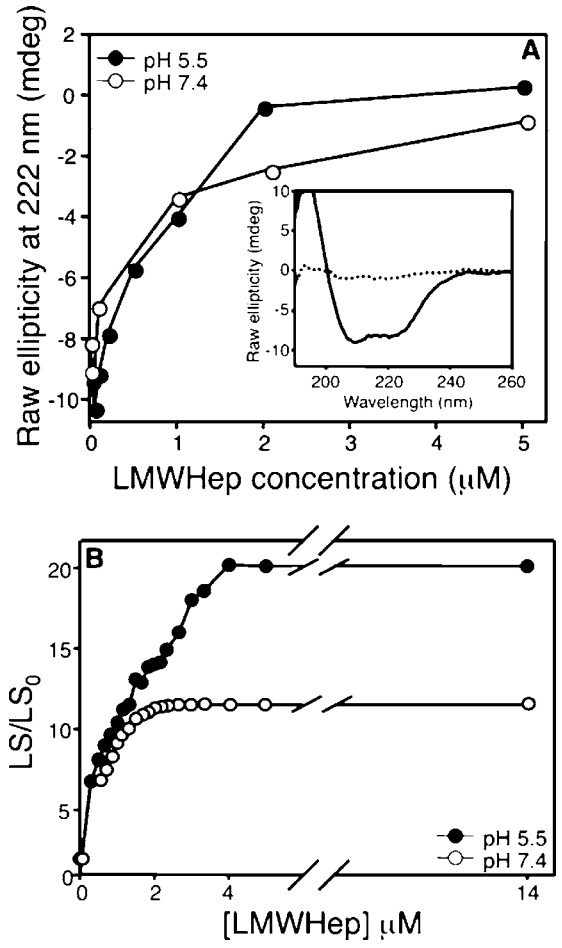

Figure 2. Effect of heparin on rPrP 23-231 secondary structure and light scattering. CD raw ellipticity measured at 222 nm for rPrP 23-231 (30 μM) (A) and relative light scattering (2 μm) (B) in the presence of different concentrations of heparin at pH values of 7.4 and 5.0, 6 s after mixing. The figure inset in (A) shows the CD spectra of rPrP 23-231 (—) and rPrP 23-231 + 5 μM LMWHep (···) at pH 7.4. The CD spectra were recorded at 25 °C with 0.01 cm circular path length cells. Experiments were performed in 10 mM Tris and 100 mM NaCl (pH 7.4) or 10 mM sodium acetate buffer and 100 mM NaCl (pH 5.5).

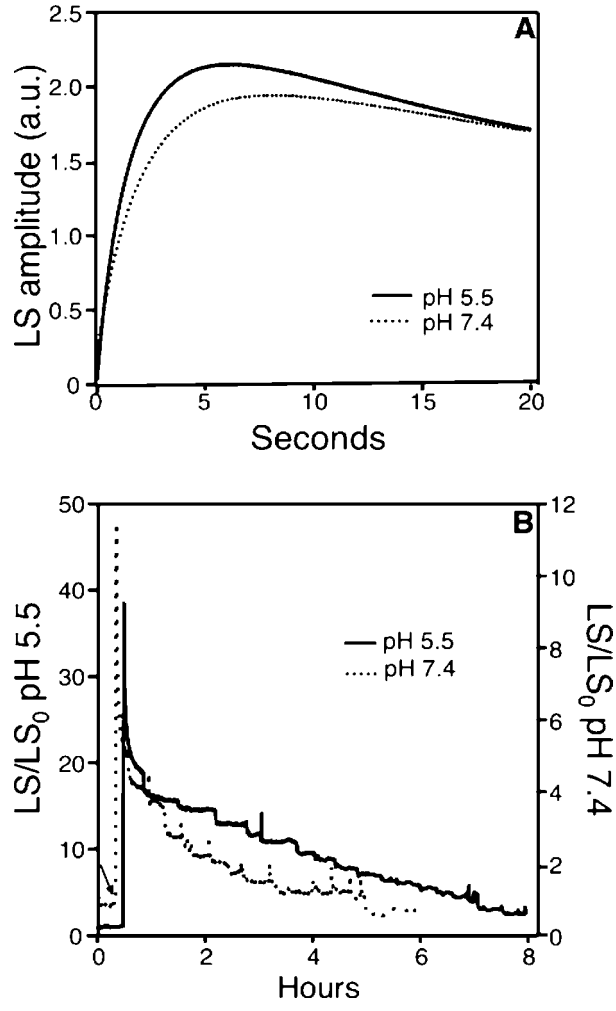

Figure 3. Kinetics of rPrP 23-231 interaction with LMWHep. Light scattering amplitude from fast (A) and slow kinetic (B) experiments. rPrP 23-231 (2.0 μM) and LMWHep (4.0 μM, A) or (2.0 μM, B). The arrow indicates the point of heparin dilution into the buffer (B). All experiments were performed in 50 mM Tris and 100 mM NaCl (pH 7.4) or 10 mM acetate and 100 mM NaCl (pH 5.5).

(Figure 3A), followed by a decrease after 6 s of the reaction. To evaluate the reversal in the effect of LMWHep after 6 s, an equimolar concentration of heparin was added to a solution of pre-equilibrated rPrP 23-231 at pH 5.5 or 7.4. LMWHep induced an immediate increase in light scattering, leading to values corresponding to the formation of large aggregates, especially at pH 5.5 (Figure 3B). This effect was followed by a slow decrease in intensity to near-initial values, suggesting a reorganization process after six to eight hours (Figure 3B). We also observed this effect using far-UV CD spectroscopy. Immediately after dilution of LMWHep into buffer, the ellipiticity values decreased at both pH values (Figure 4A). Moreover, 12 hours later, the protein native structure returned at pH 7.4 but not at pH 5.5 (Figure 4B). This difference could result from part of the protein content remaining aggregated at pH 5.5. To examine whether LMWHep and PrP continued to interact after disaggregation, we labeled LMWHep with fluorescein isothiocyanate FITC and measured its binding to PrP at pH 7.4 by fluorescence anisotropy over time (Figure 4C). We found an increase in anisotropy values after the addition of rPrP 23-231 to the sample. This effect was due to an interaction between both molecules and sample aggregation. After sample disaggregation, the anisotropy values remained higher than those of free LMWHep

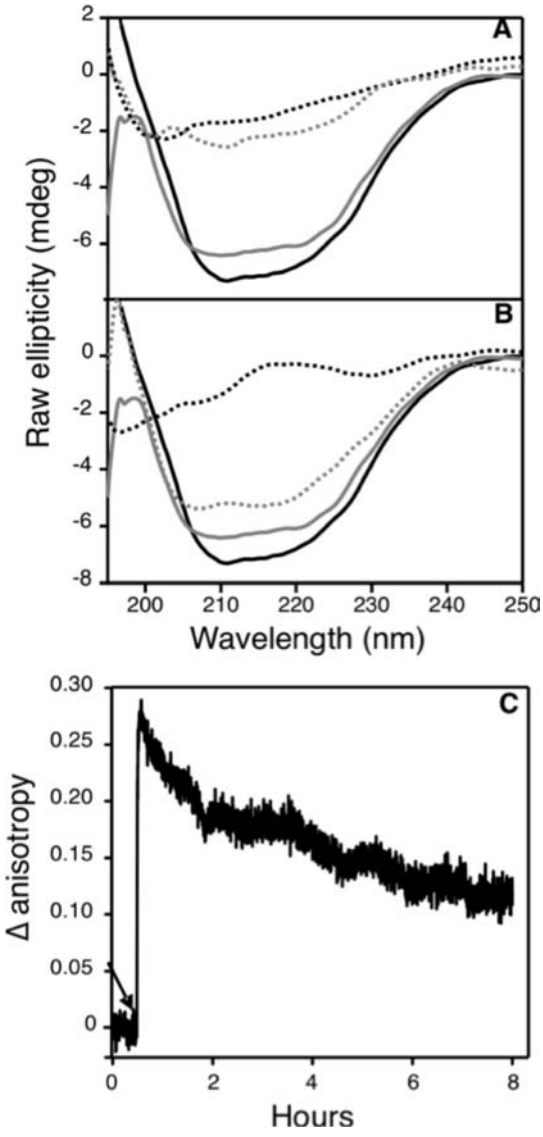

Figure 4. Effect of LMWHep and its interaction after disaggregation. CD spectra of free 30.0 μM rPrP 23-231 and in the presence of LMWHep (1:1) 6 s (A) and 20 h (B) after mixing. rPrP 23-231 at pH 5.5 (—), rPrP 23-231 at pH 7.4 (—), rPrP 23-231 + LMWHep at pH 5.5 (···), rPrP 23-231 + LMWHep at pH 7.4 (···) for (A) and (B). CD spectra were recorded at 25 °C with 0.02 cm circular path length cells. Fluorescein-labeled LMWHep anisotropy (2.0 μM) at pH 7.4 was measured as a function of time (C). The arrow indicates the moment of rPrP 23-231 (2.0 μM) dilution into the buffer. All experiments were performed in 50 mM Tris and 100 mM NaCl (pH 7.4) or 10 mM acetate and 100 mM NaCl (pH 5.5).

(Figure 4C), showing that this molecule was still interacting with PrP after this period of time. In experiments like those in Figure 3, we were able to fit the light scattering amplitudes during the first six seconds and the last eight hours by single and double exponential functions, respectively. These fittings provided the observed rate constants (k_{obs}) (Table 1), and we also obtained k_{obs} values for the first six seconds based on tryptophan fluorescence amplitudes (ΔF). The disaggregation process was approximately three orders of magnitude slower than the aggregation process, presenting a two-component kinetic process (Table 1).

Determination of Dissociation Constants and Number of Binding Sites. We performed a fast kinetic experiment using fluorescence to investigate the number of binding sites and the equilibrium dissociation constant of LMWHep binding to murine prion protein at pH values of 7.4 and 5.5. Representative kinetic traces of the tryptophan fluorescence changes are shown in Figure 5 (inset). The fluorescence amplitudes were higher at pH 5.5 than at 7.4. Based on fitting eq 1 to these data (R^2 = 0.99), apparent dissociation constants were 31.5 ± 11.7 nM (n = 3, mean ± SE) for pH 5.5 and 120.3 ± 4.9 nM for pH 7.4. The numbers of binding sites found, based on the n value, were 1.1 at pH 7.4 and 2.1 at pH 5.5.

NMR Analyses of the Complex Formed by the Prion Protein and LMWHep. NMR analyses of $rPrP^C$ at pH 4.5 and 5.5 have shown that the N-terminus is highly flexible and unstructured; by contrast, the C-terminal region has a well-structured globular domain that is rich in α-helices.[4,5] We recorded $^1H-^{15}N$ heteronuclear single quantum correlation (HSQC) spectra of rPrP 23-231 in the presence or absence of LMWHep at pH 5.5 and 7.4 (Figure 6) to obtain detailed information about the binding induced changes in protein structure. The 2D [^{15}N,^1H] HSQC spectra usually give one cross peak for each amide group in the molecule (except for proline). According to the rPrP 23-231 sequence, 288 HN cross peaks were expected in the 2D [^{15}N,^1H] HSQC. For unbound protein samples, we found approximately 260 cross peaks with good resolution. Next, LMWHep was added, and a 2D [^{15}N,^1H] HSQC spectrum of the remaining soluble complex was recorded after the binding reaction reached equilibrium (20 h later). A comparison of the spectra revealed the superposition of most peaks at both pH values, indicating that binding to LMWHep caused no drastic changes in protein folding (Figure 6A and B). Nevertheless, there were a few chemical shift differences in peaks between the free and complex spectra. We could assign some peaks corresponding to amino acids from the C-terminus for both pHs (Figure 6C). The result showed a greater number of chemical shift differences at pH 5.5 than at 7.4 (Figure 6C). Comparing with the known tridimensional structure of the prion protein, residues that showed higher chemical shift differences are colored in red, and residues that showed minor chemical shift differences are colored in gray (Figure 6D). Furthermore, there are differences in the spectra of rPrP 23-231 bound to LMWHep at different pHs (red contours). This is most dramatic in the region between 7.8−8.2 ppm in the ^1H dimension and 124−127 ppm in the ^{15}N dimension (Figure 6A and B green arrowheads). Note that most of the changed peaks are unique for each pH, and since they appear only upon binding of LMWHep, it indicates a different mode for heparin binding in each condition studied. This spectral range is mostly populated by many amide cross peaks of an unfolded polypeptide backbone (Figure 6A and B). These additional peaks can be explained by a drastic change in the chemical environment of some residues that may be directly involved in the interaction with heparin, a change in the dynamics of the polypeptide chain upon binding of this GAG, or both of these two possibilities. A polypeptide chain in a dynamic status, where the chemical exchange rate is close to the chemical shift difference between the states, can present broad cross peaks that do not build up in the spectrum. Whether the chemical exchange is very fast or is slow compared to the chemical shift difference of the states, it is possible to observe a signal in the spectrum or even several additional signals representing each conformational state of the protein.[47] The additional peaks found for rPrP 23-231 bound to LMWHep at both pH values (Figure 6A and B) suggest that this GAG induces either a new stable conformation or states of

(47) Binsch, G. *J. Am. Chem. Soc.* **1969**, *91*, 1304–1309.

Table 1. Observed Rate Constants for Fast and Slow Kinetics[a]

		aggregation	disaggregation			
		ΔLS	fast phase ΔLS		slow phase ΔLS	
sample	pH	k_{obs} (s^{-1})	k_{1obs} (s^{-1})	amp	k_{2obs} (s^{-1})	amp
rPrP23-231:LMWHep (1:1)	5.5	0.42	0.98×10^{-2}	71%	0.51×10^{-3}	29%
	7.4	0.44	0.60×10^{-2}	80%	0.25×10^{-3}	20%
rPrP23-231:LMWHep (1:2)	5.5	0.74	0.48×10^{-2}	63%	0.58×10^{-4}	37%
	7.4	0.54	0.38×10^{-2}	69%	0.63×10^{-4}	31%

[a] For fast kinetic experiments (aggregation) we used a single exponential equation to obtain rate constants (k_{obs}). Slow kinetic (disaggregation) showed two apparent phases, and we used a double exponential equation to fit this data. The rate constants from fast (k_{1obs}) and slow phases (k_{2obs}) are shown with their respective amplitudes (amp), expressed as a percentage of the total amplitude of each sample (pH 5.5 and 7.4). Values are mean of three experiments.

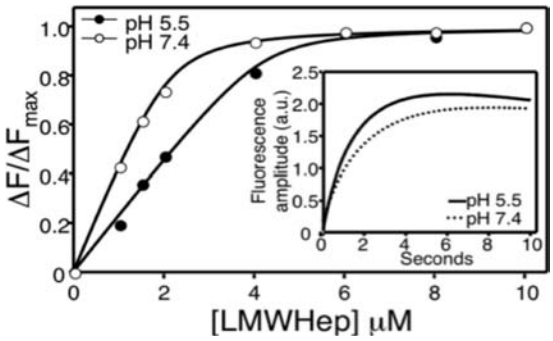

Figure 5. Stopped-flow fluorescence measurements at pH 7.4 and 5.5. Different LMWHep concentrations were mixed with 2 μM rPrP 23-231 (final concentration after mixing). The tryptophan fluorescence signal (excitation at 295 nm) was measured as a function of time for each concentration. The figure inset shows an example of the signal obtained with 4 μM LMWHep. The fluorescence amplitudes are plotted as a function of LHMHep concentration in the main panel, and the curve was obtained by fitting eq 1 to the data, as described in the Materials and Methods. Experiments were performed in 50 mM Tris and 100 mM NaCl (pH 7.4) or 10 mM acetate and 100 mM NaCl (pH 5.5).

slow or very fast chemical exchange for a number of residues. The soluble complex showed to have the same general folding at both pH values (Figure 6A and B), reinforcing that the CD spectroscopy results (Figure 4B) were due to differences in protein solubility.

Investigation of the Heparin Binding Sites of rPrP 23-231. The PrP N-terminus is important for PrP^C function and pathogenesis[48−50] as well as for rPrP aggregation.[51] Some evidence has suggested that the N-terminal region of PrP is the binding site for GAGs.[31,38,52,53] Based on PrP fragments or synthetic peptides, other investigators have reported GAG interactions with other protein sites, including C-terminal regions.[37,54] There is ongoing debate about which residues are important for the interaction. Therefore, using anisotropy measurements we investigated the interaction between LMWHep and rPrP Δ51-90, a murine PrP mutant lacking the octapeptide region (Figure 7). Increasing concentrations of heparin did not induce any significant changes in rPrP Δ51-90 anisotropy at pH 7.4, showing the importance of this region for the heparin−protein interaction at neutral pH values. By contrast, an interaction occurred at pH 5.5, suggesting the existence of another heparin-binding site along the prion sequence (Figure 7A). Furthermore, we observed this interaction by monitoring the light scattering of an rPrP Δ32-121 sample in the presence of LMWHep. In this experiment, there was an increase in light-scattering values only at pH 5.5 (Figure 7B), similar to the results obtained from anisotropy measurements with the rPrP Δ51-90 construct. Some authors have suggested the importance of histidine residues for the interaction between the prion protein and sulfated polysaccharides.[31,55] Histidine is the only amino acid that can act as a proton donor/acceptor at physiological pH.[56] To investigate the importance of histidine for the interaction with LMWHep, rPrP 23-231 samples were treated with DEPC, and the effect of LMWHep was monitored by light scattering. As shown in Figure 7C, LMWHep was not able to induce protein aggregation after DEPC treatment, indicating that this amino acid and regions containing this amino acid are crucial for the PrP:Hep interaction. When DEPC-modified rPrP 23-231 was treated with hydroxylamine, the covalent modification was reverted (see the Supporting Information, Figure S1).

LMWHep Binding to rPrP Suppresses RNA-Induced Aggregation. When PrP interacts with RNA, it forms a complex with distinct characteristics that influence its stability and propensity to convert into the scrapie conformation. Nucleic acid molecules are candidate adjuvants in the conversion of PrP^C into PrP^{Sc} and are known to induce aggregation and conformational changes in the prion protein.[17,20,23,57] We previously found that RNA extracted from cultured neuroblastoma cells can induce the formation of toxic aggregates of rPrP 23-231; we also showed that this interaction occurs through the N-terminal region of the protein (residues 51-90 only) at pH 7.4.[20] Therefore, we performed experiments to determine whether the formation of a soluble LMWHep−PrP complex could affect the PrP−RNA interaction. Light-scattering measurements were performed to evaluate the susceptibility of the LMWHep−PrP complex to RNA-induced aggregation (Figure 8).

RNA (N2a) induced aggregation of the protein alone, but it did not have the same effect on the LMWHep−PrP complex (Figure 8). This result suggests that these two anionic ligands bind to the same site of the PrP protein. However, LMWHep

(48) Zanusso, G.; Farinazzo, A.; Prelli, F.; Fiorini, M.; Gelati, M.; Ferrari, S.; Righetti, P. G.; Rizzuto, N.; Frangione, B.; Monaco, S. *J. Biol. Chem.* **2004**, *279*, 38936–38942.
(49) Lawson, V. A.; Priola, S. A.; Wehrly, K.; Chesebro, B. *J. Biol. Chem.* **2001**, *276*, 35265–35271.
(50) Lawson, V. A.; Priola, S. A.; Meade-White, K.; Lawson, M.; Chesebro, B. *J. Biol. Chem.* **2004**, *279*, 13689–13695.
(51) Frankenfield, K. N.; Powers, E. T.; Kelly, J. W. *Protein Sci.* **2005**, *14*, 2154–2166.
(52) Chen, S. G.; Teplow, D. B.; Parchi, P.; Teller, J. K.; Gambetti, P.; Autilio-Gambetti, L. *J. Biol. Chem.* **1995**, *270*, 19173–19180.
(53) Shyng, S. L.; Lehmann, S.; Moulder, K. L.; Harris, D. A. *J. Biol. Chem.* **1995**, *270*, 30221–30229.
(54) Cortijo-Arellano, M.; Ponce, J.; Durany, N.; Cladera, J. *Biochem. Biophys. Res. Commun.* **2008**, *368*, 238–242.
(55) Taubner, L. M.; Bienkiewicz, E. A.; Copie, V.; Caughey, B. *J. Mol. Biol.* **2010**, *395*, 475–90.
(56) Markley, J. L. *Acc. Chem. Res.* **1975**, *8*, 70–80.
(57) Deleault, N. R.; Lucassen, R. W.; Supattapone, S. *Nature* **2003**, *425*, 717–720.

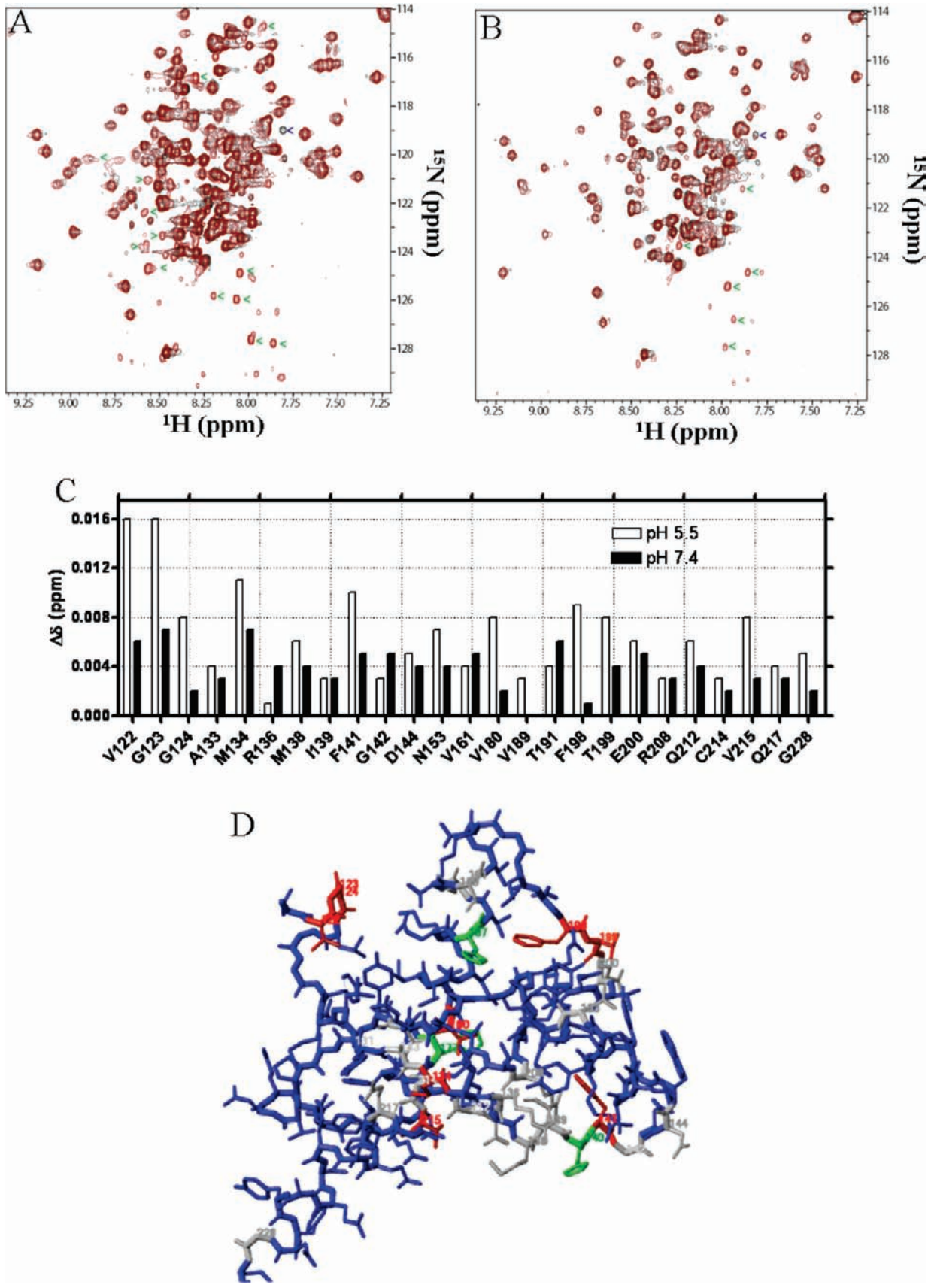

Figure 6. Effect of heparin on prion protein structure and its pH dependence. Superimposed 2D [^{1}H,^{15}N] HSQC spectra of free rPrP23-231 (black contours, collected with 8 scans) and heparin-bound rPrP23-231 (red contours, collected with 220 scans) at pH 5.5 (A) and pH 7.4 (B). Green arrowheads show cross peaks found only in heparin-bound rPrP 23-231 spectra, and blue arrowheads show cross peaks found only in free rPrP 23-231 spectra. (C) Chemical shifts differences of C-terminal identified residues at both pHs. (D) Structure of the prion protein (PDB ID: 1XYX). The protein backbone is shown with thicker bonds. Nonidentified residues in the 2D [^{1}H,^{15}N] HSQC spectra are shown in blue. Residues with small chemical shift differences are colored in gray, and residues with significant chemical shift differences are colored in red. Histidine residues are colored in green.

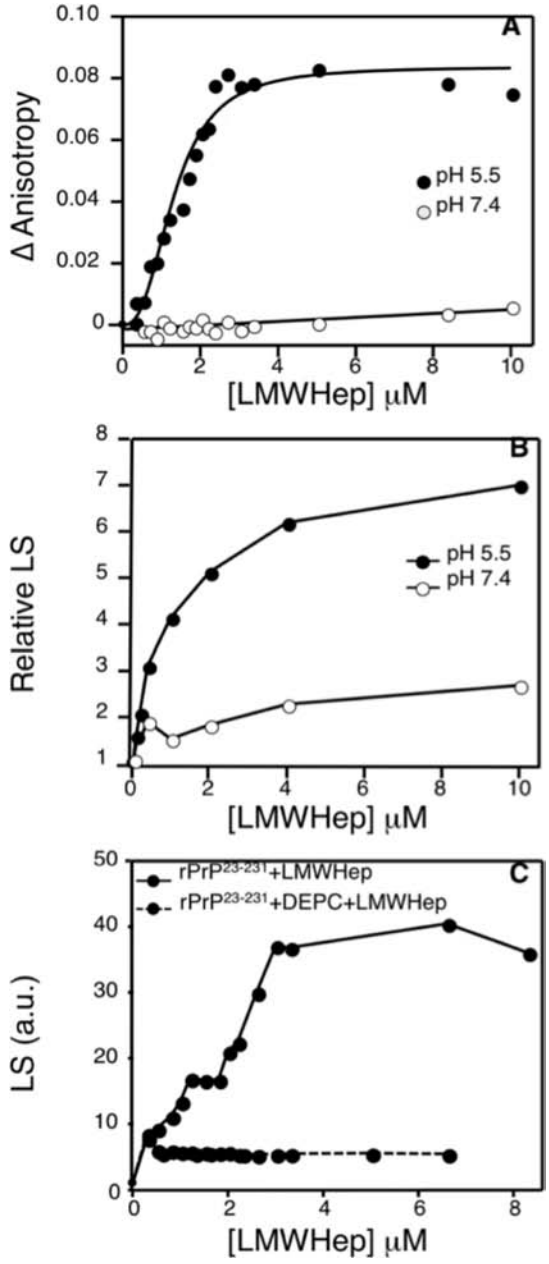

Figure 7. Importance of the N-terminus and histidine residues for the LMWHep interaction. Increasing concentrations of LMWHep were added to 2 μM rPrP Δ51-90 or Δ32-121 at pH 7.4 and 5.5. Binding was monitored by tryptophan fluorescence anisotropy of rPrP Δ51-90 at 280 nm (A) and relative light scattering of rPrP Δ32-121 (B) at 90° (excitation: 320 nm; scattering scanned from 300 to 340 nm). (C) rPrP 23-231 sample (2 μM) was incubated with DEPC (10 mM) at pH 5.5, and after 30 min, LMWHep aliquots were added to the sample (···). Light scattering of the nontreated sample in the presence of LMWHep is shown as the positive control (—).

was not able to revert N2aRNA−PrP aggregates once they were formed (see the Supporting Information, Figure S3). Another possibility that cannot be excluded is that binding to LMWHep changes the rPrP conformation, hindering the RNA-binding site and thus preventing this molecule to exert its effects on the rPrP. Thus, the LMWHep molecule prevents the aggregation induced by neuroblastoma RNA, indicating its potential use as antiprion compound.

Discussion

A change in the conformation of PrP^C from an α-helix-rich protein to a predominantly β-sheet form (PrP^{Sc}), followed by aggregation, is the main cause of TSEs.[6,7] PrP^{Sc} propagates itself, inducing PrP^C to acquire the PrP^{Sc} conformation through an autocatalytic process; however, this simple conversion reaction is not efficient in vitro.[58] Therefore, the accumulation of toxic prions is believed to involve the participation of various cellular cofactors, including glycosaminoglycans. The main GAG shown to be involved in pathogenesis is membrane-bound heparan sulfate.[24,25,59]

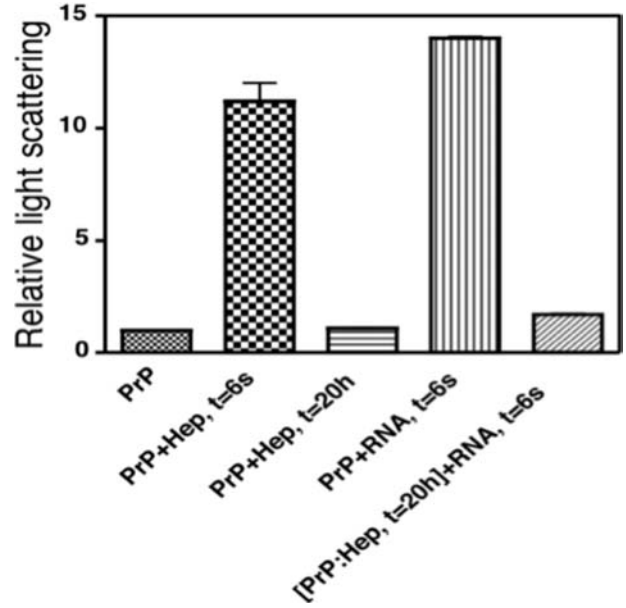

Figure 8. N2aRNA effect on the rPrP 23-231:LMWHep complex. Light scattering of rPrP at 1 μM, rPrP:LMWHep (1:1) 6 s after mixing, rPrP:LMWHep (1:1) 20 h after mixing, rPrP:RNA 6 s after mixing, and preincubated [rPrP:LMWHep (1:1), t = 20 h] + RNA 6 s after mixing. Results are expressed relative to rPrP 23-231 light scattering. Experiments were performed in 50 mM Tris and 100 mM NaCl (pH 7.4). The error bars indicate the standard error of three experiments.

Heparin, which resembles the sequences found in heparan sulfate, is widely used therapeutically and is readily available in large quantities; therefore, it is often used as a model for heparan sulfate interactions. Heparin has been shown to interact with some prion constructs and to induce the formation of oligomeric complexes at acidic pH values.[31,36] Here, we investigated the interaction between the recombinant murine prion protein and LMWHep and the structural features forming the basis of this association. The conversion of prion protein is believed to occur at the cell surface or in endocytic or recycling vesicles,[10−12,60] and the interaction between heparan sulfate proteoglycan and PrP^C is important in trafficking between compartments.[61] Therefore, we chose to conduct all of our experiments at pH values of 5.5 and 7.4 to resemble lysosomal and cellular fluid pH values, respectively. There is substantial evidence that a transient PrP intermediate conformer populated at mildly acid pH may be a direct precursor of the PrP^{Sc} oligomer.[62] We showed that LMWHep is able to bind murine

(58) Hill, A. F.; Antoniou, M.; Collinge, J. *J. Gen. Virol.* **1999**, *80* (Pt 1), 11–14.
(59) Hijazi, N.; Kariv-Inbal, Z.; Gasset, M.; Gabizon, R. *J. Biol. Chem.* **2005**, *280*, 17057–17061.
(60) Marijanovic, Z.; Caputo, A.; Campana, V.; Zurzolo, C. *PLoS Pathog.* **2009**, *5*, e1000426.
(61) Cheng, F.; Lindqvist, J.; Haigh, C. L.; Brown, D. R.; Mani, K. *J. Neurochem.* **2006**, *98*, 1445–1457.
(62) Apetri, A. C.; Maki, K.; Roder, H.; Surewicz, W. K. *J. Am. Chem. Soc.* **2006**, *128*, 11673–11678.

rPrP at both pH values but with an apparent heparin:protein ratio of 1:1 at pH 7.4 and 2:1 at pH 5.5 (Figure 5). This result indicates the presence of an additional interaction site at pH 5.5. There is clearly an increased affinity at acidic pH. Andrieviskaia et al.[36] reported a K_d value of 73.45 nM for the interaction between bovine recombinant prion protein and heparin (mw = 12 000) at pH 5.5. Here, we measured K_d value of 31.5 ± 11.7 nM for pH 5.5, suggesting that size of heparin or the origin of the recombinant protein can influence the affinity.

The protein-only hypothesis is the more widely accepted theory for prion protein conversion.[9] However, crude brain homogenates and polyanions (including heparan sulfate) have been shown to generate more efficient conversion than purified prion proteins alone.[23,63,64] These studies suggest that other molecules may promote important changes in the prion protein structure, thereby inducing or facilitating conversion. Some authors have monitored these structural changes by far-UV CD spectroscopy,[32,36] but protein aggregates are known to cause artifacts due to differential light scattering and absorption flattening. These factors distort the magnitude of the CD spectra and decrease the signal/noise ratio.[65−67] We observed a decreased CD ellipticity induced by LMWHep (Figure 2A), but changes in light scattering (Figure 2B) indicate that the structural information has been masked by protein aggregation, even in the absence of protein precipitation. For this interaction, CD spectroscopy would not report protein conformational changes efficiently.

Protein−water interactions are important for folding stability because a native conformation depends on the exposure of hydrophobic surfaces to the aqueous milieu.[68] PrP^C has a large solvent accessible area and regions that exchange rapidly with bulk water.[69,70] Our fast kinetic measurements showed that the LMWHep interaction with rPrP 23-231 led to an increase in fluorescence and light-scattering values (Figures 3A and 5). However, this was a transient effect, as both signals decreased six to eight seconds after mixing; moreover, the light-scattering values returned to initial values after several hours (Figure 3B). Aggregation occurred much more rapidly than disaggregation (Table 1). These data suggest that the interaction with LMWHep induces local conformational changes, through the alignment of tryptophan residues and exposure of a hydrophobic surface, as was observed for pentosan polysulfate,[55] leading to self-association, decreased solvent accessibility, and an increased intensity of intrinsic tryptophan fluorescence (Figure 5). Flexible protein regions must mediate these intermolecular interactions. This phenomenon seems to be followed by a stabilization process, which is a period with varied folding behavior, until equilibrium is reached. Disaggregation leads to increased protein hydration and, consequently, to decreased fluorescence intensity.

Next, we investigated whether this transient aggregation and binding to heparin would induce conformational changes that lead PrP^C to PrP^{Sc}. Our CD experiments showed that the protein α-helical content after disaggregation returned to values similar to that of the free protein at pH 7.4 (Figure 4B). NMR spectra of the soluble complex showed a general tertiary structure that was very similar to that of the free protein (Figure 6A and B). Although most of the differences in the chemical shifts between the free and heparin-bound rPrP 23-231 samples were small, we observed additional cross peaks in a spectral range usually populated by signals from the unfolded region of the protein, suggesting that this region may become less disordered due to heparin binding. In addition, we could identify some C-terminal residues based on the sequence specific resonances. This analysis showed that there are some differences in chemical shift changes when rPrP 23-231 is bound to LMWHep in different pHs. Specifically, we have identified the residues V122, G123, G124, M134, F141, V180, F198, T199 and V215 (Figure 6C and D). Additional changes could not be ruled out in the crowded area of the 2D [^{1}H,^{15}N] HSQC, which is very difficult to distinguish alterations in chemical shifts. In fact, some additional peaks in this area can be from amino acids from the C-terminus that is binding to LMWHep. Together, differences in the chemical shifts corresponding to residues from the N- and C-termini indicated that binding to LMWHep affects the structure of different protein regions, and the effect is dependent on pH.

Yin et al.[38] showed that deletion of the first 12 amino acids of human rPrP inhibits its interaction with GAGs, and they also suggested that additional octapeptide repeat insertions (consensus sequence of PHGGGWGQ) generate a more exposed N-terminus that enhances the GAG interaction. Using fragments or synthetic peptides, other authors have reported that this octapeptide region and other regions are the main components that mediate the GAG interaction,[31,37,55] but whether the behavior of these peptides is representative of the full-length protein is unknown. In this work, we used an rPrP mutant lacking residues 51-90 (octapeptide repeat) (Figure 7A). LMWHep did not interact with rPrP Δ51-90 at pH 7.4, showing that this is the only interaction site at neutral pH, congruent with the observed stoichiometry of 1:1 (LMWHep:PrP) at pH 7.4. These results are consistent with the observation[53] that the PrP region between residues 25 and 91 (including the octapeptide repeat region) is sufficient for PrP binding to heparan sulfate proteoglycans moieties on N2a cells; however, our data contradict those of Gonzales-Iglesias et al.,[31] who observed an interaction with bovine PrP(63-94) only at acidic pH values. We found two interaction sites for rPrP 23-231 at acidic pH values (Figure 5). To investigate the presence of additional interaction sites at acidic pH, we followed the interaction of rPrP Δ51-90 at pH 5.5 (Figure 7A). Although there was no interaction between this mutant and LMWHep at pH 7.4, we observed binding at pH 5.5, with an apparent ratio of 1:1 (LMWHep:PrP), indicating that there are two interaction sites at acidic pH (the octapeptide region and another region responsible for binding to rPrP Δ51-90 at pH 5.5) in the full-length protein (Figure 7A). To determine the second binding site, we used another rPrP mutant lacking most of the N-terminus (rPrP Δ32-121) (Figure 7B) and found that LMWHep was able to induce the oligomerization of this mutant only at pH 5.5, suggesting that this second binding region is either within the first N-terminal amino acids (agreeing with Yin et al.)[38] or near the protein's C-terminal domain.

(63) Lucassen, R.; Nishina, K.; Supattapone, S. *Biochemistry* **2003**, *42*, 4127–4135.
(64) Saborio, G. P.; Permanne, B.; Soto, C. *Nature* **2001**, *411*, 810–813.
(65) Kelly, S. M.; Jess, T. J.; Price, N. C. *Biochim. Biophys. Acta* **2005**, *1751*, 119–139.
(66) Litman, B. J. *Biochemistry* **1972**, *11*, 3243–3247.
(67) Castiglioni, E.; Abbate, S.; Longhi, G.; Gangemi, R.; Lauceri, R.; Purrello, R. *Chirality* **2007**, *19*, 642–646.
(68) Silva, J. L.; Vieira, T. C.; Gomes, M. P.; Bom, A. P.; Lima, L. M.; Freitas, M. S.; Ishimaru, D.; Cordeiro, Y.; Foguel, D. *Acc. Chem. Res.* **2010**, *43*, 271–9.
(69) Cordeiro, Y.; Kraineva, J.; Ravindra, R.; Lima, L. M.; Gomes, M. P.; Foguel, D.; Winter, R.; Silva, J. L. *J. Biol. Chem.* **2004**, *279*, 32354–32359.
(70) De Simone, A.; Dodson, G. G.; Verma, C. S.; Zagari, A.; Fraternali, F. *Proc. Natl. Acad. Sci. U.S.A.* **2005**, *102*, 7535–7540.

Scheme 1. Schematic View of rPrP 23-231 Interaction with LMWHep[a]

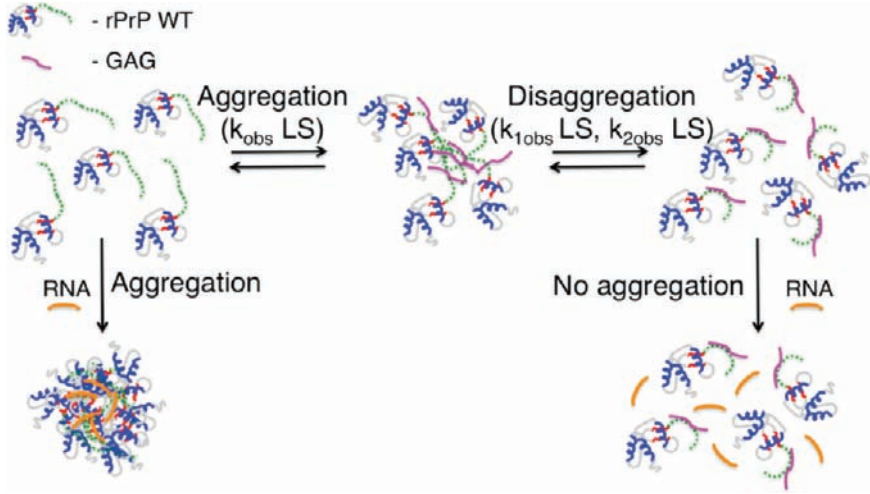

[a] rPrP 23-231 has a globular C-terminal domain (blue, α-helices; red, *β*-sheet), and a highly flexible N-terminal domain (green) that assumes different spatial positions. This region would bind LMWHep (pink) and other glycosaminoglycans (GAGs), favoring self-association and leading to protein aggregation. The protein−protein contacts formed would be weak, followed by protein disaggregation. After disaggregation, rPrP 23-231 remains interacting with LMWHep showing a very similar fold to the free monomer, with no scrapie-like conformation, but with a less flexible N- terminus domain. RNA molecules (orange) can bind rPrP 23-231 at its N-terminal leading to irreversible aggregation. However, RNA is not able to induce aggregation with LMWHep−PrP complex.

The conformational properties of prion protein are known to be modulated by pH.[71,72] Changes that increase the exposure of the N-terminus and of normally hidden motifs could lead to a new binding site at acidic pH. Alternatively, histidine residues, such as His155 and His187, could be protonated, an event that happens at approximately pH 5.5.[71,72] We used DEPC to probe the role of histidine residues, and we observed that this reagent was able to abolish the interaction of rPrP with LMWHep (Figure 7C). DEPC modifies nucleophiles such as amine, imidazole, thiol and guanidine groups, producing carbethoxyl derivatives. It specially carbethoxylates not only histidyl residues but also tyrosyl, seryl and lysyl residues. Lysine modification happens preferentially from pH 6.0 to 8.0, and the histidine's reactivity increases in the presence of acetate buffers.[73] Hydroxylamine removes the ethoxyformyl group from modified histidine but not from ethoxyformyl-lysine residues.[74] Hydroxylamine treatment was able to revert the modifications induced by DEPC on rPrP 23-231 (see the Supporting Information, Figure S1). Moreover, the mass spectrum of rPrP 23-231 after reaction with DEPC showed an increase of 585 Da suggesting the modification of eight from the total of nine histidines (data not shown). These results suggest that the second binding region does not include the first 12 amino acids of the N-terminus, which lacks histidine residues. The chemical shift differences found for rPrP 23-231 C-terminal residues (Figure 6C) are in accordance with the possibility of the existence of two binding sites for heparin at pH 5.5 and only one at pH 7.4, suggesting that the second binding site lies within the globular region of the prion protein. Moreover, many residues identified so far that presents greater chemical shift difference at pH 5.5, including Val122, Gly123, Gly 124, Phe198, and Thr199 are found closer (9.2−13.0 Å of their Cα) to histidine 187 in the protein's 3D structure.

Sulfated polysaccharides can have seemingly paradoxical effects, either blocking[75−79] or stimulating[23,24,32,58] PrP^{Sc} formation. The antiprion effect of free GAGs may occur due to competition for binding to PrP with cellular GAGs. However, free GAGs can stimulate cell-free conversion.[32] In this work, we showed that LMWHep is able to bind a full-length prion protein and induce its aggregation, but this was a transient effect that generated little modification of the protein structure (explaining lack of conversion stimulation by antiprion compounds). Although these changes in protein structure are important, they are not sufficient to induce disease (Scheme 1). Other molecules, such as the scrapie agent, other proteins, or a nucleic acid, may be needed. Our findings that the soluble complex of LMWHep−rPrP is resistant to aggregation induced by RNA (Figure 8) demonstrate the flexibility of the PrP structure. Depending on the RNA molecule, the interaction with PrP might lead to the formation of toxic aggregates that are resistant to proteolysis (similar to the scrapie conformation).[20] Scheme 1 depicts how complex formation with LMWHep would block RNA-induced aggregation. Therefore, the GAG interaction might be more protective than deleterious to the PrP^{C} conformation.

Cellular GAGs, most frequently found as proteoglycan side chains, are immobilized at the cell membrane, as is PrP^{C}. Aggregation induced by GAG in the cell-membrane environment would be a sporadic event, given the spatial restriction,

(71) Swietnicki, W.; Petersen, R.; Gambetti, P.; Surewicz, W. K. *J. Biol. Chem.* **1997**, *272*, 27517–27520.
(72) Calzolai, L.; Zahn, R. *J. Biol. Chem.* **2003**, *278*, 35592–35596.
(73) Langella, E.; Improta, R.; Crescenzi, O.; Barone, V. *Proteins* **2006**, *64*, 167–177.
(74) Mendoza, V. L.; Vachet, R. W. *Mass Spectrom. Rev.* **2009**, *28*, 785–815.
(75) Caughey, B.; Raymond, G. J. *J. Virol.* **1993**, *67*, 643–650.
(76) Gabizon, R.; Meiner, Z.; Halimi, M.; Ben Sasson, S. A. *J. Cell Physiol.* **1993**, *157*, 319–325.
(77) Ladogana, A.; Casaccia, P.; Ingrosso, L.; Cibati, M.; Salvatore, M.; Xi, Y. G.; Masullo, C.; Pocchiari, M. *J. Gen. Virol.* **1992**, *73* (Pt 3), 661–665.
(78) Schonberger, O.; Horonchik, L.; Gabizon, R.; Papy-Garcia, D.; Barritault, D.; Taraboulos, A. *Biochem. Biophys. Res. Commun.* **2003**, *312*, 473–479.
(79) Ouidja, M. O.; Petit, E.; Kerros, M. E.; Ikeda, Y.; Morin, C.; Carpentier, G.; Barritault, D.; Brugere-Picoux, J.; Deslys, J. P.; Adjou, K.; Papy-Garcia, D. *Biochem. Biophys. Res. Commun.* **2007**, *363*, 95–100.

degree and transience of the effect observed at pH 7.4. Furthermore, heparan sulfate proteoglycans may be important for infectivity by concentrating PrP^{C} for conversion and being involved in PrP^{Sc} incorporation into cells.

Acknowledgment. We thank Dr. Martha M. Sorenson for carefully reading the manuscript; Dr. Narcisa L. Cunha e Silva for analysis by transmission electron microscopy; and Dr. Kurt Wüthrich and Dr. Simone Hornemann for providing mPrP(121-231) assignment. This work was supported by grants from Conselho Nacional de Desenvolvimento Científico e Tecnológico (CNPq), Instituto Nacional de Ciência e Tecnologia de Biologia Estrutural e Bioimagem (CNPq INCT Program), and Fundação Carlos Chagas Filho de Amparo à Pesquisa do Estado do Rio de Janeiro (FAPERJ). Y.C. acknowledges a grant from ABC-UNESCO-L'Oréal.

Supporting Information Available: Saturation curve with DEPC and hydroxylamine effect on rPrP 23-231 modification. Transmission electron microscopy analysis of LMWHep−PrP aggregates. Further experimental data about LMWHep effect on protein aggregation induced by RNA. This material is available free of charge via the Internet at http://pubs.acs.org.

JA106725P